HEUSLER COMPOUNDS: A BRIEF REVIEW AND SOME THEORETICAL STUDIES

Fábio S. da Rocha, Gilberto Luís F. Fraga, Delmar E. Brandão
Instituto de Física
UFRGS - Porto Alegre-RS
Celso Marques da Silva
Departamento de Física – CCNE
UFSM - Santa Maria-RS
Affonso A. Gomes
Centro Brasileiro de Pesquisas Físicas
Rio de Janeiro, RJ

ABSTRACT

In this review paper we briefly recall some existing experimental and theoretical work on the magnetic properties, specific heat and transport properties of pure and pseudo ternary Heusler compounds. Previous existing theoretical descriptions of the electronic structure, magnetic moment formation, coupling between moments and magnetic order, together with some work developed by the Porto Alegre Transport Group, are presented and discussed.

1. INTRODUCTION

Solid State community is celebrating the first century of research on Heusler compounds. Metallurgical studies on ternary intermetallic alloys, involving non magnetic elements, which resulted in the discovery of the first synthetic ferromagnets started with F. Heusler in the late 1898.

Heusler's first publication in this field appeared in 1903 and reported the study of the Cu-Mn-Z (Z = Al, As, Bi, B, Sn) alloys, some of which presenting ferromagnetic properties. This paper produced a big impact on the magnetism community, which started an intense effort to determine in which composition the alloys could present their best magnetic properties. Yet in 1903, Stark and Haupt published their work on Cu-Mn-Z (Z = Al, Sn), where they showed that the maxima in the magnetization of these materials occur at the approximate compositions Cu_2MnAl and Cu_6Mn_3Sn. The Cu-Mn-Sn system was studied again by Ross and Gray in 1910, when a higher maximum in magnetic intensity was discovered near the composition Cu_2MnSn.

After these experiments, the important question was to determine the crystalline structure of these alloys. The difficulty lied in distinguishing between Cu and Mn sites using available X-ray devices. The works of Person (1928), Potter (1929) indicated cubic symmetry with Al atoms forming a face centered cubic superlattice as in DO_3 (Fe_3Al type structure). On the other hand it was observed the extreme dependence of the magnetic properties on the thermal treatment of the alloys. Nowadays, it is well established that a good number of compounds only attain the correct crystalline structure at elevated temperatures, requiring a quenching process in order to obtain such structure at root temperature.

The definitive work on the structure of Heusler alloys was carried out by Bradley and Rogers (1934). Using X-rays of different wave

lengths (radiation from Fe, Cu and Zn targets) they were able to show that the Mn and Cu atoms were also ordered in a $L2_1$ crystalline structure. After this point, Heusler materials were considered ternary intermetallic compounds, that obey X_2TZ stoichiometric composition and $L2_1$ structure.

Whence established the crystalline structure, the next crucial question concerned to the origin of the magnetic properties of these materials. From the neutron diffraction experiments it was found that a large localized magnetic moment of about $4\mu_B$ was observed on Mn atoms.

The existence of such a large localized magnetic moment intrigated theorist about its origin and coupling mechanism. Differently from rare-earth metals and classical transition metal ferromagnets, these compounds exhibited in some cases a sort of intermediate behaviour. Studies of the coupling between localized magnetic moments, without assuming direct interaction, were possible only after the application of the indirect Ruderman-Kittel-Kasuya-Yosida (RKKY) interaction, at the beginning assuming strictly localized moments and after that, with Caroli and Blandin [1], using the resonance introduced by Friedel. In all these works, the case of Mn magnetic moments has been considered in compounds of the type X_2MnZ.

A very large number of Heusler compounds series, defined by the majority element X (X = Cu, Ni, Pd, or another) have been studied. Inside each X series with Mn, and by changing the sp element (Z), one may obtain Heusler compounds with quite different magnetic properties. The role of sp elements in defining the magnetic properties of these materials was found very important. As an example, let us quote Pd_2MnIn which is antiferromagnetic as compared with Pd_2MnSn, which is ferromagnetic.

In what concerns the Mn magnetic moment, only recently, using powerful APW band calculation techniques, Kubler and collaborators have shown that the local spin dependent band structure of Mn is composed

by a completely filled majority spin band and an almost empty minority spin band, [2]. Thus, through this calculation, the origin of the local moment on Mn, received a simple and convincing explanation.

In this review paper we intend to discuss, after the presentation of some experimental results, the description of the interaction between magnetic moments in pure and pseudo ternary Heusler compounds.

2. CRYSTALLINE STRUCTURE

Heusler intermetalic ternary compounds were first defined as obeying the stoichiometric composition X_2TZ, where X and T are transition elements and Z is an sp atom. This definition has changed with time and nowadays materials with the composition XTZ are referred as Heusler compounds too. The reason for that lies on the crystalline structure of these materials. This structure is best described in terms of four interpenetrating fcc sublattices A,B,C and D, as shown in figure 1. At the stoichiometric composition X_2TZ, in chemically ordered compounds, X atoms occupy sites A and C, B sites are occupied by T atoms and the Z occupy D sites. This arrangement corresponds to the Strukturbericht type $L2_1$. When partial disorder occurs, with T and Z atoms occupying both B and D sites, one has a B2 type arrangement. In the case of XTZ ordered compounds, the C sites are unoccupied and the arrangement is said to be of $C1_b$ type [3]. Partial disorder may occur in these compounds, like the one mentioned above, involving T and Z components, giving rise to the C1 type of arrangement.

It is interesting to mention here that the binary intermetallic DO_3 compounds, which obey X_3Z stoichiometric composition, are chemically ordered materials. The DO_3 crystalline structure may be considered as a particular case of the $L2_1$, in which sites B are also occupied by X atoms. This fact allows to write their formula unit as X_2XZ, stressing the Heusler-like character of these compounds.

3. PREPARATION

3.1.Metallurgical Processes

Most of the Heusler compounds studied have been prepared by arc melting techniques, under an argon atmosphere. Quality tests show that, even using a remelting procedure, it is necessary to apply an annealing process in order to obtain well ordered samples. The time as well as the temperature to be used in this annealing process is a function of the material's composition. Melting temperature gives an upper limit for a faster homogenizing process, that should be followed by another annealing period, conducted at a temperature defined by the phase diagram of the compound. Phase diagrams are available only for a few Heusler compounds, so that most of them are prepared empirically. For those compounds for which the $L2_1$ phase occurs at high temperatures, a fast cooling process has to be applied. In this case one may expect the presence of some crystalline defects, that may vary as a function of sample's preparation.

3.2. Quality Tests

The Heusler phase determination is usually performed by using x-ray powder diffraction techniques. A good number of single crystal Heusler compounds have been prepared and had their chemical and magnetic order determined by neutron diffraction experiments.

The presence, in the diffraction spectra, of the (111) line, identifies the $L2_1$ structure; this line is absent in the B2 phase, but for both, the proeminent spectral line is the (220) one.

Beyond phase determination, diffraction experiments allow lattice parameter calculation, as well as the study of the degree of order of the

samples and the identification of spurious phases eventually present. These procedures are presently made by Rietveld refining methods [4].

3.3. Crystalline defects

Changes in the physical properties of Heusler compounds may be induced by the introduction of crystalline defects. Cold work, high pressure and thermal effects (fast cooling processes) are the main origin of atomic disorder, dislocations, planar defects like antiphase domain boundaries (which affect the magnetization strength). Among the more used techniques in the study of crystalline defects one may mention transmission electron microscopy and scanning electron microprobe.

3.4. Phase transitions

The occurrence in nature of single phase ordered materials is not a trivial fact. Most Heusler compounds are high temperature materials, which may be frozen by a quenching process, to keep their $L2_1$ structure at lower temperatures.

The crystallographic transition, from the chemically ordered $L2_1$ phase to the partially disordered $B2_1$, has been the subject of some differential thermal analysis (DTA) experiments. The involved transition temperatures have been determined only for around ten Heusler compounds. The existing theoretical approach to describe these crystallographic transitions has bem developed using the Bragg-Williams approximation. For a small number of compounds, martensitic phase transitions do occur [5].

4. ELECTRONIC STRUCTURE

Historically the first published calculation on the electronic structure of Heusler compounds was made by Ishida et al. in 1978 [6] using spin polarized symmetrized augmented plane wave method applied to

Cu_2MnAl compound. In the majority of the referred band calculations, a characteristic property of the density of states of Heusler compounds is to exhibit the existence of three distinct valleys. The highest energy valleys indicate the location of the bonding and antibonding states. The antibonding states are located above the highest energy valley and are almost empty. The bonding states are located below the intermediate energies. This behaviour seems to be a general feature of these compounds, independently of the T atoms [7].

For a large number of Heusler compounds, the Fermi energy may be located in an energy region with decreasing density of states. This fact, together with the assumption of a rigid band model, explains the variation of physical properties connected to the density of states along a sequence of compounds, like X_2TZ, Z = In, Sn, Sb.

Heusler compounds Fe_2TSi, which may be considered as obtained from the DO_3 compound Fe_3Si (by introducing transition impurities T, substituting Fe atoms) present a strong selective substitution effect. This effect follows from the detailed structure of the local density of states associated to the majority (Fe) element sites and to the minority transition elements (T) sites. From these densities, one estimates which energy is lower and thus how the site selectivity of Fe_2TSi compounds appears.

One of the most complex questions concerning the Heusler compounds with Mn, was the origin of the localized moment behaviour of these Mn atoms. The localized nature of the moments, in previous theoretical works was an assumption to simplify the calculations. In 1983 J. Kübler et al., using a self-consistent spin polarized band calculation, showed that the site projected majority spin band was almost completely filled. On the contrary, the minority spin band was shown to be almost an empty band, thus justifying the occurrence of a local moment at the Mn site. This theorem by Kübler and collaborators has been demonstrated for a number of Heusler compounds, [2].

Finally, from the electronic structure calculations, a very peculiar result has been obtained: some $C1_b$ compounds show the existence of a gap around the Fermi energy. In the case of the compounds FeVSb, NiZrSn and NiUSn, the band calculation shows that these materials present a non magnetic semiconductor behaviour. In the case of NiUSn at high temperatures this material becomes a metal with AF ordering. For the ferromagnetic compounds NiMnSb and PtMnSb, the gap occurs in the minority spin band.

It is interesting to observe that alloys exhibiting the DO_3 crystalline structure, a particular case of the $L2_1$ with stoichiometry given by X_3Z (X_2XZ), show very peculiar magnetic properties. In the case, for instance, of Fe_3Si, it is possible to observe two different behaviours of Fe magnetic moments. In Fe sites which have eight Fe nearest neighbours, the magnetic moment is almost the same as in pure Fe matrix. On the contrary, in sites where Fe has four Fe and four Si nearest neighbours, its magnetic moment becomes the half of the value at the other Fe sites. This shows the importance of the specific neighborhood of an Fe site, since the specificity of hoppings (d-d or d-p) affects the local band width and consequently the magnetism.

5. MAGNETIC PROPERTIES

5.1. Origin of the magnetic moments

In many papers of the literature concerning the discussion of the origin of the magnetic properties of Heusler compounds, for the sake of simplicity, the magnetic moments of Mn are described by localized spins. Historically, the large distance between Mn atoms motivated the theoretical description in terms of localized Mn moments coupled via the conduction electron gas. As briefly described in the Electronic Structure section, the origin of a localized Mn magnetic moment follows from the band calculation in

terms of a completely filled majority spin band and an almost empty minority spin band. This result applies to a significant set of compounds of the type X_2MnZ.

There are however some specific cases where the transition element T component of X_2TZ is a rare earth, for which the existence of a local moment is true.

Among the ferromagnetic Heusler comounds there are some examples of mixed behaviour (eg. Co_2MnZ). One expects an itinerant character for the Co 3d electrons and a localized behaviour for Mn atoms as described above. This is a quite interesting situation, since Co moments follow from the Hartree-Fock description including the effective field arising from the Mn local moments, and thus a mixed magnetic behaviour occurs.

Another situation is provided by compounds Mn_2WSn, Fe_2TiAl, Co_2TiAl and others, in which the transition element T do not form a magnetic moment. These are typical cases of itinerant magnetism.

The last possibility concerns the compounds in which the magnetic order is associated to a T element different from Mn, for example Ru_2FeSn. One expects in this case a quite different situation as compared to the X_2MnZ Heusler compounds with X=Pd, Cu, Au. Again one may say that an itinerant magnetism is induced by the 3d element, which eventually magnetizes also the X element.

The above comments about some experimental results show that band structure calculations still remain to be performed to clarify these situations.

5.2. Interaction between magnetic moments

In what concerns the theoretical studies of the interaction between magnetic moments, four main lines are present in the literature.

In the first one, the Heusler compounds are considered to exhibit only a localized magnetic moment, assumed to be located at the T transition element component, the coupling being mediated by the conduction electrons via the usual RKKY interaction.

Secondly, following Caroli-Blandin [1] and Price's picture [8], magnetic moments are described by Friedel resonant scattering model, from which one calculates the interaction energy. In the case of the existence of magnetic moments in both X and T atoms (thus allowing direct interaction), a mixed treatment is necessary, since the itinerant electrons require a Hartree-Foch treatment with the extra effective magnetic field associated to the localized spins.

The third approach, known as the Blandin-Campbell picture [9] is a improved version of the RKKY description of the coupling between local moments to include the scattering of conduction electrons by a potential associated to the departure from charge neutrality at the sp sites. In the case of sp neighbours in the Periodic Table: Pd_2MnIn (antiferromagnetic) and Pd_2MnSn (ferromagnetic).

The fourth line is provided by pure itinerant electron magnetism mentioned at the end of the above section. This itinerant magnetism behaviour requires a more complex treatment of the temperature dependence of the magnetization; a functional integral approach is required to estimate the transition temperatures [10].

5.3. Two sublattice model for the magnetic properties

In this paragraph we present a generalization of Blandin-Campbell [8] approach for the magnetic order in Heusler compounds in terms of impurity perturbations within the coherent potential approximation (CPA), [11].

The Heusler compound is divided into two sublattices A and B; A is associated to the X atoms and the B corresponds to sites occupied by the Z and T atoms. In the absence of d-p hopping between X and Z atoms, the local and independent densities of states associated to each sublattice are constructed from the dispersion relations $\varepsilon_k^{\alpha}(\alpha = d, p)$. For compounds like Ni_2MnZ or Co_2MnZ, where Z is a sp atom, at the A sublattice one expects a dominating d-character density of states. For the sublattice B, on the contrary, one assumes an almost pure p-density of states, with larger band width as compared to the d one. Finally a hopping or hybridization exists between these d and p states.

We thus describe the resolvent for this two sublattice system by a 2x2 matrix, in close analogy to Laves phase compounds [12]. The resolvent reads:

$$g_k(z) = \begin{pmatrix} z - \varepsilon_k^d & t_k^{dp} \\ t_k^{pd} & z - \varepsilon_k^p \end{pmatrix}^{-1} \tag{1}$$

In this equation one assumes that ε_k^d and ε_k^p are associated only to hoppings between sites in the A and B sublattices respectively; in the elements t_k^{pd} and t_k^{dp}, we include hoppings between neighbouring d and sp atoms and in this sense it is a sort of hybridization. By matrix inversion one obtains the resolvents for the sublattice A:

$$g_k^{AA}(z) = \frac{z - \varepsilon_k^p}{(z - \varepsilon_k^d)(z - \varepsilon_k^p) - t_k^{dp} t_k^{pd}} \tag{2}$$

The propagators in real space, more adequate for the calculations, are obtained by Fourier transformation:

$$g_{ii'}^{AA}(z) = \sum_k e^{ik(R_i - R_{i'})} g_k^{AA}(z) \tag{3}$$

In conclusion, if the dispersion relations ε_k^{α} and the hybridizations t_k^{dp}, t_k^{pd} are known, the real space propagators can be numerically calculated by summing over the Brillouin zone. The propagator for the B sublattice is simply obtained replacing ε_k^{p} by ε_k^{d} in (2).

The next and central step of this calculation is to obtain the indirect coupling between Mn localized moments and then determining the transition temperature using the mean field approximation. At this point, let us introduce some convenient notation: the localized Mn moments occupy sites R_i of the Heusler lattice. We denote by $R^{N,\alpha}(R_i)$ the location of the next neighbours N in sublattice α (A or B) of a Mn atom at site R_i; a sum over N means a sum over these neighbours. As mentioned above, there exists an hybridization between the Mn 3d states with the remaining ones coming from the X and Z atoms. These effects are qualitatively included in our formulation, by assuming that the spin-conduction electron interaction is local, like in the usual derivation of the RKKY [13]. In the present case, we extend this interaction to couple Mn local spins to conduction electrons at neighbouring sites. In this way the effective field reads now:

$$H^{\alpha}_{R^N(R_i)} = J^{\alpha}_{Mn} S^{z}_{Mn}(R_i) \qquad (4)$$

Since the exchange interaction is small as compared to the α involved band widths, we assume that the first Born approximation to Dyson's equation is adequate. This field acting in the α sublattice, introduces a non local term in the equation for the α propagator. The perturbed propagator for a given spin σ reads:

$$G^{\alpha\alpha}_{R_m R_m,\sigma}(z) = g^{\alpha\alpha}_{R_m R_m}(z) - \sigma \sum_{R^N(R_i)} g^{\alpha\alpha}_{R_m R^N(R_i)} \left[J^{\alpha}_{Mn} S^{z}_{Mn}(R_i) \right] g^{\alpha\alpha}_{R^N(R_i) R_m} \qquad (5)$$

This expression gives the diagonal locator at site R_m in presence of a local moment at site R_i. From this locator one can derive the magnetization $m^{\alpha}_{R_m}$ at the site R_m of sublattice α. Using the imaginary theorem and at zero temperature, one gets:

$$m^{\alpha}_{R_m} = \frac{2}{\pi}\int^{\varepsilon_F} \mathrm{Im}\left[\sum_{R^N(R_i)} g^{\alpha\alpha}_{R_m R^N(R_i)} g^{\alpha\alpha}_{R^N(R_i) R_m}\right] J^{\alpha}_{Mn} S^{z}_{Mn}(R_i) \qquad (6)$$

where ε_F is the Fermi level of the compound, determined in such a way that the sum of the occupation numbers given by the local density of states, associated to X and Z atoms, is the adequate one.

The next step is to calculate the indirect interaction between the Mn moments at R_i and R_j; to do that one needs the magnetizations at the neighbours of R_j, replacing R_m in (6) by $R^N(R_j)$, summing over them and multiplying by $(J^{\alpha}_{Mn}) S^{z}_{Mn}(R_j)$. The result for the interaction involving the α sublattice is:

$$E^{\alpha}_{\mathrm{int}}(R_i, R_j) = \frac{2}{\pi}\int^{\varepsilon_F} \mathrm{Im}\left[\sum_{R^N(R_j), R^N(R_i)} g^{\alpha\alpha}_{R^N(R_j) R^n(R_i)} g^{\alpha\alpha}_{R^N(R_i) R^N(R_j)}\right]$$

$$\left[(J^{\alpha}_{Mn})^2 S^{z}_{Mn}(R_i) S^{z}_{Mn}(R_j)\right] \qquad (7)$$

The total interaction is obtained summing over α:

$$E_{\mathrm{int}}(R_i, R_j) = J_{eff}(R_i, R_j) S^{z}_{Mn}(R_i) S^{z}_{Mn}(R_j) \qquad (8)$$

where

$$J_{eff}(R_i, R_j) = \sum_{\alpha} \left[J_{Mn}^{\alpha} \right]^2 F^{\alpha}(R_i, R_j) \tag{9}$$

and

$$F^{\alpha}(R_i, R_j) = \frac{2}{\pi} \int^{\varepsilon_F} \left[\sum_{R^X(R_j), R^X(R_i)} g^{\alpha\alpha}_{R^X(R_j) R^X(R_j)} g^{\alpha\alpha}_{R^X(R_i) R^X(R_j)} \right] \tag{10}$$

For the case of ferromagnetic order, by the use of the mean field approximation, we estimate the Curie temperature in terms of sums over the lattice points:

$$k_B T_c = \left(S_{Mn}^z \right)^2 \sum_j J_{eff}(R_i, R_j) \tag{11}$$

Up to this point only ternary Heusler compounds have been considered. Many experiments have been performed in alloys, were X or Z atoms are replaced by a given concentration c of X′ or Z′ atoms. For this particular two sublattice systems we can follow the same method used in Laves phase compounds [12], provided homothetic bands are assumed. Since the CPA approximation restores translational invariance, equations (2) are valid provided one introduces the self-energy Σ. Using CPA, the equation (1) is replaced by:

$$g_k^{AA}(z) = \begin{bmatrix} z - \sum(z) - \varepsilon_k^d & t_k^{dp} \\ t_k^{pd} & z - \varepsilon_k^p \end{bmatrix}^{-1} \tag{12}$$

in the case of selectively alloying the A sublattice. Following the same procedure for a two sublattice system, described in reference [14] one obtains for the self-energy:

$$(1-c)\frac{\varepsilon_0^x - \sum(z)}{1-\left(\varepsilon_0^x - \sum(z)\right)g_{00}^{XX}(z)} + c\frac{\varepsilon_0^{imp} - \sum(z)}{1-\left(\varepsilon_0^{imp} - \sum(z)\right)g_{00}^{XX}(z)} = 0 \quad (13)$$

where ε_0^{imp} being the impurity level and ε_0^x is the center of the d-band. A similar result is obtained when the impurities occupy the Z sublattice.

Once determined the self energy, the same steps from (4) to (9) adopted for the pure Heusler compounds, can be used to calculate $J_{eff}(R_i, R_j; c)$ as shown in figure 2. The Mn magnetic moment is obviously supposed unaltered by the disorder within this model and for calculating the critical temperature only the concentration dependence of the effective exchange coupling is relevant. Using (12) it is possible to estimate the transition temperature (11) as a function of the impurity concentration, see figure 3.

5.4 Types of observed magnetic order

The magnetic order and the measured transition temperature, for a large number of Heusler compounds, are reported in the literature. The great majority of these compounds exhibit ferromagnetic order and only a small part of them show antiferromagnetism or other kinds of order.

Still more scarce are those showing non trivial magnetic order eg Ag_2TbAl and Au_2MnAl both cycloidal spiral antiferromagnetic. Following Doniach [12], one obtains, within the random phase approximation, that the local moment induced magnetization M(Q) is given in terms of the independent electron susceptibility χ (Q), the Fourier transform of the exchange interaction J(Q) and the Coulomb interaction by:

$$M(Q) = \frac{(J(Q))^2 \chi(Q)}{1 - U\chi(Q)} \quad (14)$$

From this result it follows that the induced periodicity of the magnetization corresponds to the Q value that makes $1-U\chi(Q)$ closer to zero. Thus if this condition occurs for for Q=0 one gets ferromagnetism, if it happens for Q=π we have antiferromagnetism and to others Q values an incommensurate period occurs. One should calculate numerically, for the band structure of the corresponding compound, the susceptibility $\chi(Q)$ with the wave vector Q [15]. This criterion furnishes the type of magnetic instability.

Other compounds show Pauli paramagnet behaviour (temperature independent), Curie-Weiss paramagnetic behaviour and also diamagnetism eg. Cu_2NiSn , Cu_2LuIn , Au_2YIn. Less common Van Vleck paramagnetism has been detected in Cu_2SmIn and Ag_2SmIn compounds.

Recently the existence of weak metallic ferromagnetism, with a high Curie temperature has been reported for the following Heusler compounds with X = Pd, Cu, T = Ti, V and Z = Al, In, Sn, [16]. For these compounds only non magnetic atoms, differently from Mn or rare earth are present and this defines an interesting problem to explain their itinerant magnetism. In the specific case of Pd_2TiAl, the ferromagnetic moment per formula unit is very small 0,2 μ_B, but with Curie temperatures larger than 900K. It can be suggested that the difference in magnetic behaviour (ferromagnetic/ paramagnetic) of these materials may be explained in terms the Landau-Ginsburg free energy for a coupled two subsystem. Again assuming two sublattice magnetizations associated to Pd and to Ti, these are defined by $\vec{m}$ and the Landau-Ginsburg coefficients a and A of am^2 and A M^2 of the free energy, together with the intersublattice coupling c$\vec{m}\cdot\vec{M}$. We assume that for C=0 the free energy minimization gives $\vec{m}$= $\vec{M}$ =0 For C $\neq$ 0 the total free energy G is given by:

$$G = am^2 + bm^4 + AM^2 + BM^4 + c\,\vec{m}.\vec{M} \tag{15}$$

Minimization respect to the order parameters furnishes the values of the magnetic order, which now are associated to the inter sublattice coupling. The high value of the transition temperature requires however a functional integral description [9].

To conclude, the magnetic properties are, among all the physical properties of Heusler compounds, the most extensively studied. After these theoretical remarks, let us briefly comment about some transport properties in Heusler compounds; here we restrict ourselves to the role of impurities and magnetic moments in these transport properties.

6. ELECTRICAL RESISTIVITY

6.1. Scattering mechanisms

The electrical transport properties of magnetic Heusler compounds are thought to be associated mainly to the conduction by sp electrons. Scattering of these electrons, come from the lattice vibrations and interactions with the spin magnetic moments. At low temperatures collective spin modes are excited (magnons) which are an important contribution to the resistivity. As the temperature increases, single particle excitations start to play a role. The scattering of the electrons may involve both elastic and inelastic terms and the relative importance of the different types of scattering, will vary with temperature. We thus start discussing these mechanisms for some specific cases.

6.1.1. Scattering mechanisms present in all metals

The Residual resistivity ρ_0 (ρ at T = 0) is associated to electronic scattering due to impurities, crystal defects and it is essentially temperature independent. In the particular case of Heusler ternary compounds X_2TZ, the magnitude of ρ_0 may be connected to the degree of chemical order of the compound. However, these materials allow the selective substitutions of impurities in different lattice sites, as for example $X_2T(Z_{(1-x)}Z'_x)$. In this way it is possible to study the almost continuous changes in the residual resistivity. In the literature we may find, among others, the cases of $Ni_2MnSn_{(1-x)}In_x$., [17] and $Cu_2MnAl_{(1-x)}Sn_x$, [18]. A possible way to study theoretically this effect is furnished by the CPA, as adapted to transport phenomena. The fact that Heusler compounds are ternary, and remembering that their structure may be described in terms of two interpenetrating substructures, suggests the use of a two sublattice model, [12]. This simple model includes different band widths for the same dispersion relation, namely ε_k and $\alpha\varepsilon_k$, together with the hybridization between the two bands. For transition metal alloys, this simple picture provided good results as compared to experiment. However, this model has nor yet been applied to transport properties in the case of Heusler compounds, thus opening another interesting research subject.

The electron-phonon scattering is one of the classical mechanisms to describe $\rho \times T$ curves. At low temperatures, as compared to the Debye temperature (θ_D), the resistivity varies as $A_{eph}T^5$ (Bloch-Gruneisen) as it has been detected, for example, in the cases of Cu_2NiSn, [19], Cu_2MnAl, [20], Ni_2MnSn, [21]. An important point is that, although magnetic in the low temperature region, the last two compounds exhibited a

predominant T^5 term. This is consistent with the high value of the ferromagnetic transition temperature. For higher temperatures respect to θ_D, one gets the linear term in T.

The electron-electron scattering furnishes a term $A_{ee}T^2$ which is in general small as compared to the other contributions. The worse case is provided by the magnetic compounds, where a T^2 contribution comes from electron-magnon interaction.

6.1.2. Scattering mechanisms present in magnetic metals

Electron-spin wave scattering occurs at low temperatures, as compared to the magnetic transition temperature. This term has the temperature variation: $A_{sw}T^2$. In some cases, for example Pd_2MnZ, with Z = In, Sn, Sb, due to the competition with the electron-phonon T^5 term, experiment furnishes at low temperatures a T^n behaviour, with $n \neq 2$.

Electron-spin interactions are observed at intermediate temperatures as compared to the magnetic transition temperature, and have been described by Kasuya [22] like terms $A_k(S-\sigma(T))(S+\sigma(T+1)$, where

is the temperature dependent magnetization. Among others, this is the case of the following compounds: Cu_2MnAl [20]. Ni_2MnSn [21] and Ni_2MnIn [23],

Electron-spin disorder resistivity, $A_{sd}S(S+1)$, temperature independent, occurring at temperatures higher than the transition temperature (ensuring the absence of short range order) [24]. For Heusler compounds this contribution has been poorly studied to our best knowledge, in particular in what concerns the impurity-spin disorder scattering.

6.2. Critical behaviour

The resistivity behaviour of ferromagnetic Heusler compounds, of the type X_2MnSn, has a large temperature interval. The resistivity (ρ) increases steadily up to the Curie temperature T_c. At $T=T_c$ there is one inflection point, and after that, the slope of the curve is considerably lower, approaching to an electron-phonon type linear behaviour. Above T_c , in the region of short range order, the change with temperature describes the decrease of the spin scattering resistivity, the asymptotic tendency to a linear behaviour corresponding to the destruction of the short range order. The critical behaviour of $d\rho / dT$ around T_c has been studied experimentally and theoretically by a few authors. The existence of a well defined and sharp cusp, around the critical temperature, reflects the homogeneity of the sample with a well defined transition temperature. Accurate resistivity measurements allows the numerical determination of $d\rho / dT$, and the critical exponent α of the specific heat. In this way, a connection can be made between two different kinds of experiments, near the transition temperature. A interesting case is provided by Pd_2MnZ, with Z = Sn, In and Al, [25].

7. SPECIFICC HEAT

In this paragraph, we briefly recall some recent experimental data concerning specific heat measurements, performed by the Porto Alegre Group on Ni_2TAl compounds with T = Ti, Zr, Hf, V, Nb and Ta. Together with these experiments, we have made a linear muffin-tin orbital (LMTO) calculations for the electronic structure of these compounds, [26].

We start describing the procedure to analyze our experimental data shown in figure 4 for the specific heat; the data are presented in a C/T versus T^2 plot. A linear trend is observed for all compounds up to about 5K

The dotted curves in figure 4 were obtained by considering the least squares fit of the experimental points from about 3.2K up to the end of the linear behavior, using the equation:

$$C(T) = \gamma T + \beta T^3 \tag{16}$$

where γ and β are the electronic and phononic coefficients respectively. The values of γ and θ_D obtained using (16) in the above mentioned temperature range are shown in the Table II. The θ_D coefficient is related to the limit T $\rightarrow$ 0 to the Debye temperature θ_D by the expression:

$$\beta = \frac{12}{5}\pi^4 Rn\theta_D^{-1} \tag{17}$$

where n is the number of atoms per formula unit (n = 4 for Heusler compounds) and R is the gas constant.

The continuous curves in figure 4 where obtained by considering a least squares fit of the experimental points from 3.2K to near 10.3K, using the equation:

$$C(T) = \gamma T + (1-p)C_D(T) + pC_E(T) \tag{18}$$

The Debye specific heat per moll is given by:

$$C_D(t) = 9nR\left(\frac{T}{\theta_D}\right)^3 \int_0^{\frac{\theta_D}{T}} \frac{y^4 \exp(y)}{\left[\exp(y)-1\right]^2} dy \tag{19}$$

and the Einstein specific heat per moll by:

$$C_E(T) = 3nR\left(\frac{\theta_E}{T}\right)^2 \left\{\exp\left(\frac{\theta_E}{T}\right) - 1\right\}^{-2} \exp\left(\frac{\theta_E}{T}\right) \tag{20}$$

where θ_E is the Einstein temperature. This term is usually associated to the existence of a flat portion of the phonon dispersion relations. In order to ensure the correct sum of normal modes, we have introduced in (18) the

weight factor p. To fit the experimental points using (18) we calculated numerically the Debye specific heat contribution in terms of the θ_D extracted from the linear part of the data. The results of this fitting procedure are presented in the Table I, where we exhibit the values of the Einstein temperatures θ_E and the weight factors p. It should be noted that the Einstein weight factors p, albeit small, induce the necessary corrections to the Debye term.

These results are shown although the compounds are non magnetic, because we have calculated the electronic density of states (see figure 5a and figure 5b) as well as estimated the lattice parameters from first principles LMTO. As it is well known, electron-phonon renormalization changes the electronic density of states; thus combining the results from the LMTO calculation with experiment, estimates of the electron-phonon interaction λ are possible and shown in Table III, as well as the calculated $a_{0(theo)}$ and experimental $a_{0(exp)}$ lattice parameters together with experimental electronic density of states $\rho_{\exp}(\varepsilon_F)$ and the calculated $\rho_{theo}(\varepsilon_F)$.

8. SUPERCONDUCTIVITY AND OTHERS PROPERTIES

Some Heusler compounds exhibit superconducting behaviour at low temperatures, [27]. Another characteristic of these materials is to show coexistence with magnetic order, in the case antiferromagnetic. We just recall that coexistence can occur only in the cases where the coherence length is large enough to accommodate enough changes in sign of the magnetization such that the total magnetic field is small enough to avoid the superconducting pair breaking. This phenomenon was described by Anderson as cryptomagnetism. Clearly for antiferromagnetic compounds, even for not too large coherence length, coexistence is already ensured,

since the total magnetization vanishes in the scale defined by the coherence length. In some cases, reentrant effects do occur, and the origin of superconductivity is usually associated to the electron-phonon interaction.

Kondo like behaviour are shown by non magnetic Heusler compound, substitutionally doped with a magnetic atoms. An example of that is given by Cu_2NiSn (which is diamagnetic) doped with Mn. One observes a minimum in the electrical resistivity as a function of temperature, this minimum changing with the concentration x of magnetic impurities.

The Curie temperature variation due to pressure has been measured in Ni_2MnIn, Ni_2MnSb, Pd_2MnIn, Pd_2MnSn, Pd_2MnSb, and also the electrical resistivity, as a function of pressure, has been observed in Pd_2MnSb, $Cu_2Mn_{0.94}In$, Cu_2MnAl, Cu_2NiSn, $Cu_2MnAl_{1-x}Sn_x$, $Cu_2MnIn_{1-x}Sn_x$ and Ag_2CeIn.

9. SPECIAL SERIES

The large spectrum of compounds obtained by changing substitutionally the X, Y, and Z components, a systematic study of period isoelectronic effects (eg, Ni_2TAl, T = Ti, Zr, Hf [26]) as well as changes in electron number (eg, Pd_2MnZ, Z = In, Sn, Sb) can be performed. It should be remembered that a large number of experiments has been performed and concerns pseudo ternary compounds. The selective substitution of X or T or Z components enables the study of the continuous variation of the physical properties associated to period (isoelectronic) or the changes in electron number.

A very interesting case of smooth transition is obtained by the substitution of Fe atoms in the Fe_3Si (DO_3 compounds), which exhibit strong selectivity effects. Substituting Fe by transition elements to the left of Fe in the Periodic Table, these atoms will be located in other Mn sites (for

example: Fe_2VSi); the transition elements to the right of Fe in the Periodic Table will occupy majority element sites (for example Fe_2CoSi, $(Fe,Co)_2FeSi$). This effect may be understood in terms of the electronic structure.

10. FINAL REMARKS AND CONCLUSIONS

In this review paper we have concentrated our attention in some of the physical properties of Heusler compounds. We insisted in the theoretical description of the magnetic properties, since as mentioned in the Introduction, magnetism was the main motivation of F. Heusler, 100 years ago, to produce these compounds. Also, the previous theoretical work shows, in a quite illustrative way, how the origin and coupling of he magnetic moments can be studied using advanced electronic structure calculations. Quite similarly to Laves phase compounds, a simple model can be adequately used to describe the origin of exchange interactions in these systems. Also, some recently discovered two sublattice metallic borocarbide superconductors, can again be described by this two band model [28]. This observation indicates that the magnetic and some superconducting properties of two sublattice compounds like Heusler, Laves and borocarbides have a common denominator in a possible simple description of their electronic structure.

BIBLIOGRAPHY

[1] B. Caroli and A. Blandin, J. Phys. Chem. Sol.27 (1966) 503.

[2] J. Kubler et al., Phys. Rev. B28 (1983) 1745.

[3] D. E. Brandão et al., Phys. Stat. Sol.(a) 139 (1993) 67; D.E. Brandão and A. A. Gomes, Phys. Stat. Sol.(a) 142 (1994) 27.

[4] H. N. Rietveld, J. Apply. Cryst. 2 (1969) 75.

[5] P. J. Webster et al., Philos. Mag. B49 (1984) 295.

[6] S. Ishida et al. J.Phys.Soc. Jap. 41 (1976) 1570.

[7] C. D. Gelatt et al., Phys. Rev. B27 (1983) 2005.

[8] D. C. Price, J. Phys F (Metal Physics) 8 (1978) 973.

[9] A. Blandin and I. A. Campbell, Phys. Rev. Lett. 31 (1973) 51.

[10] N. A. de Oliveira and A. A. Gomes, J.Mag. Magn. Mat.,114283; A. de Oliveira and A. A. Gomes, Physica Status Solidi (b), 184 (1994) 179.

[11] C. M. da Silva, D. E. Brandão and A. A. Gomes, J.Mag. Magn. Mat.,162 (1996) 107.

[12] N. A. de Oliveira and A. A. Gomes, J.Mag. Magn. Mat.,114 (1992) 175.

[13] S. Doniach, Theory of Magnetism in Transition Metals, Proc. Int. School Enrico Fermi, Course 37, Acad. Press, New .York, (1967) 125.

[14] C. M. da Silva and A. A. Gomes, An. Acad. bras. Ci, 68 (2) (1996) 139.

[15] P. A. Lindgard, B.N. Harmon and A.J. Freeman, Phys. Rev. Lett. 35 (1975) 383; J. Y. Rhee, X. Wang and B. N. Harmon, Phys. Rev. B 51 (1995) 15585.

[16] K. U. Normann et al., Sol. State. Comm. 91 (1994) 443; K. U. Neuman et al., J. Mag. Magn. Mat. 140-144 (1995) 185.

[17] G. L. Fraga et al., J. Phys. Chem. Sol. 46 (1985) 1071.

[18] J. V. Kunzler et al., J. Phys. Chem. Sol. 41 (1980) 1023.

[19] W. H. Schreiner, P.Pureur and D.E. Brandão, Phys. Stat.Sol.(a) 58 (1980) K137.

[20] F. Ogiba et al., Phys Stat. Sol (a) 66 (1981) K83.

[21] J. V. Kunzler et al., J.Phys. Chem. Sol. 40 (1979) 427.

[22] T. Kasuya, Prog. Theor. Phys. 16 (1956) 58.

[23] G. L. F. Fraga et al. Phys Stat. Sol (a) 83 (1984) K187.

[24] A. Troper and A. A. Gomes, Physica Status Solidi (b), 68 (1975).99.

[25] P. Pureur et al.,Revista Brasileira de Física 21 (1991) 179.

[26] F. S. da Rocha et al., Physica B 269 (1999) 154; W. Lin and A. J. Freeman, Phys. Rev. B45 (1992) 61.

[27] M. A. S. Boff et al.,J. Mag. Magn. Mat.,153 (1996) 135.

[28] C. M. da Silva, D. E. Brandão and A. A. Gomes, Physica C 304 (1998) 73.

Compound	$a_{0(exp)}$	γ (exp)	θ_D	θ_E	p
Ni_2TiAl	0.58948	13.38±0.12	411±4.7	95.1±2.0	0.023
Ni_2ZrAl	0.61147	13.67±0.16	278±1.5	76.6±0.4	0.030
Ni_2HfAl	0.60810	10.91±0.23	288±0.3	70.4±1.1	0.024
Ni_2VAl	0.58031	14.18±0.27	358±6.7	81.3±2.0	0.015
Ni_2NbAl	0.59755	11.03±0.14	300±1.9	75.1±0.6	0.023
Ni_2TaAl	0.59608	10.06±0.29	301±3.8	73.4±0.9	0.022

Table I: Lattice parameter a_0(nm) as obtained using the Fullprof software, electronic specific heat γ (mJ/K^2 mol), Debye (θ_D)(K) and Einstein (θ_E)(K) temperatures, obtained using equation (20).

Compound	γ (exp)	θ_D
Ni_2TiAl	13.37±0.06	410±1.7
Ni_2ZrAl	13.67±0.13	276±1.6
Ni_2HfAl	10.85±0.13	287±1.6
Ni_2Val	14.17±0.10	356±1.9
Ni_2NbAl	10.95±0.12	300±1.9
Ni_2TaAl	10.01±0.14	299±1.9

Table II: Electronic specific heat γ (mJ/K^2 mol), and Debye temperature θ_D (K) as obtained using equation (19).

Compound	a_0(exp)	a_0(theo)	$\rho_{exp}(\varepsilon_F)$	$\rho_{theo}(\varepsilon_F)$	λ
Ni_2TiAl	0.58948	0.58870	3.42 ± 0.03	2.9431	0.162
Ni_2ZrAl	0.61147	0.62121	3.49 ± 0.04	2.7066	0.289
Ni_2HfAl	0.60810	0.61182	2.79 ± 0.05	2.4000	0.162
Ni_2VaI	0.58031	0.57813	3.62 ± 0.07	2.4367	0.486
Ni_2NbAl	0.59755	0.60358	2.82 ± 0.07	1.8620	0.514
Ni_2TaAl	0.59608	0.60044	2.57 ± 0.15	1.8255	0.407

Table III: Experimental lattice parameters $a_{0(exp)}$(nm), theoretical lattice parameters $a_{0(theo)}$(nm), experimentally derived DOS, $\rho_{exp}(\varepsilon_F)$ (states/eVmo), theoretically derived DOS $\rho_{theo}(\varepsilon_F)$.(states/Ry.fu) and electron-phonon coupling parameters λ .

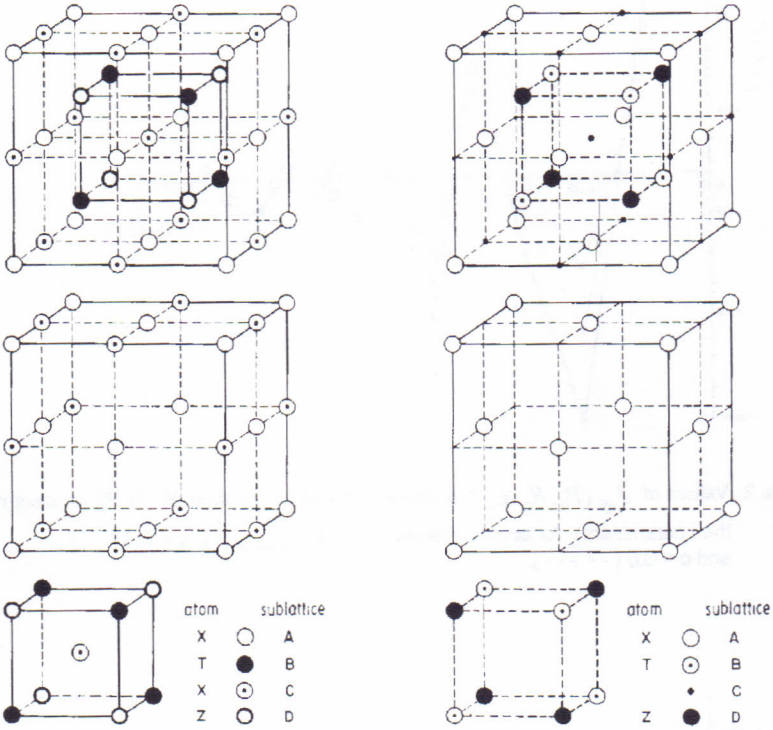

Figure 1: The crystalline structure of Heusler compounds: $L2_1$ and $C1_b$.

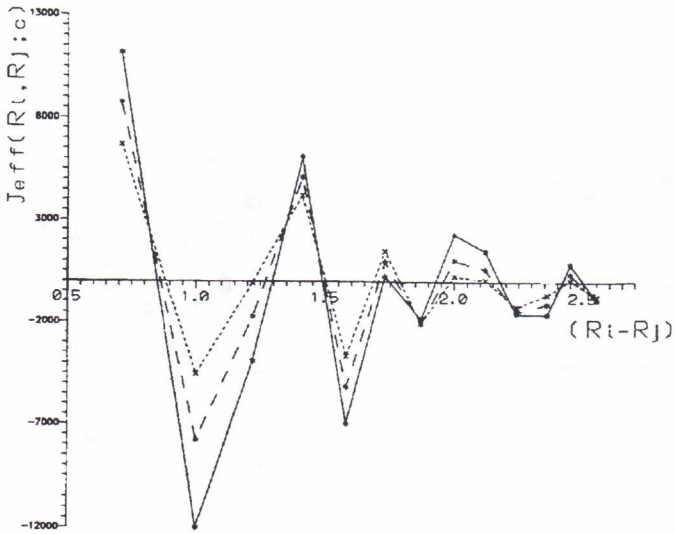

Figure 2: Values of $J_{eff}(R_i, R_j; c)$ (arbitrary units) as a function of $|R_i-R_j|$ (in units of the I parameters) for concentrations c = 0.0 (_____), c = 0.4 (__ __ __) and c = 0.8 (- - - - -).

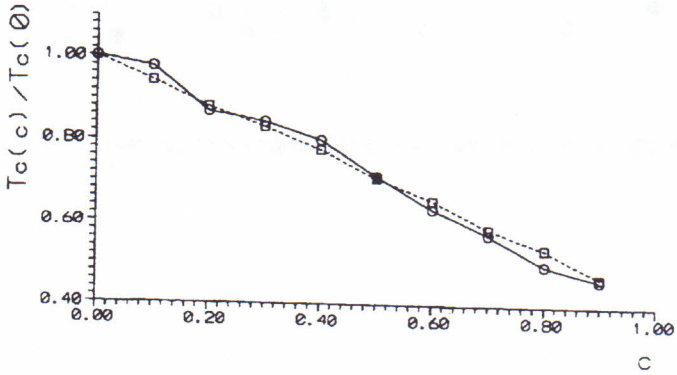

Figure 3: $T_c(c)/T_c(0)$ as a function of concentration c for the compound $Co_{1-c}Ni_cMnSn$ experimental (dotted) and theoretical (full).

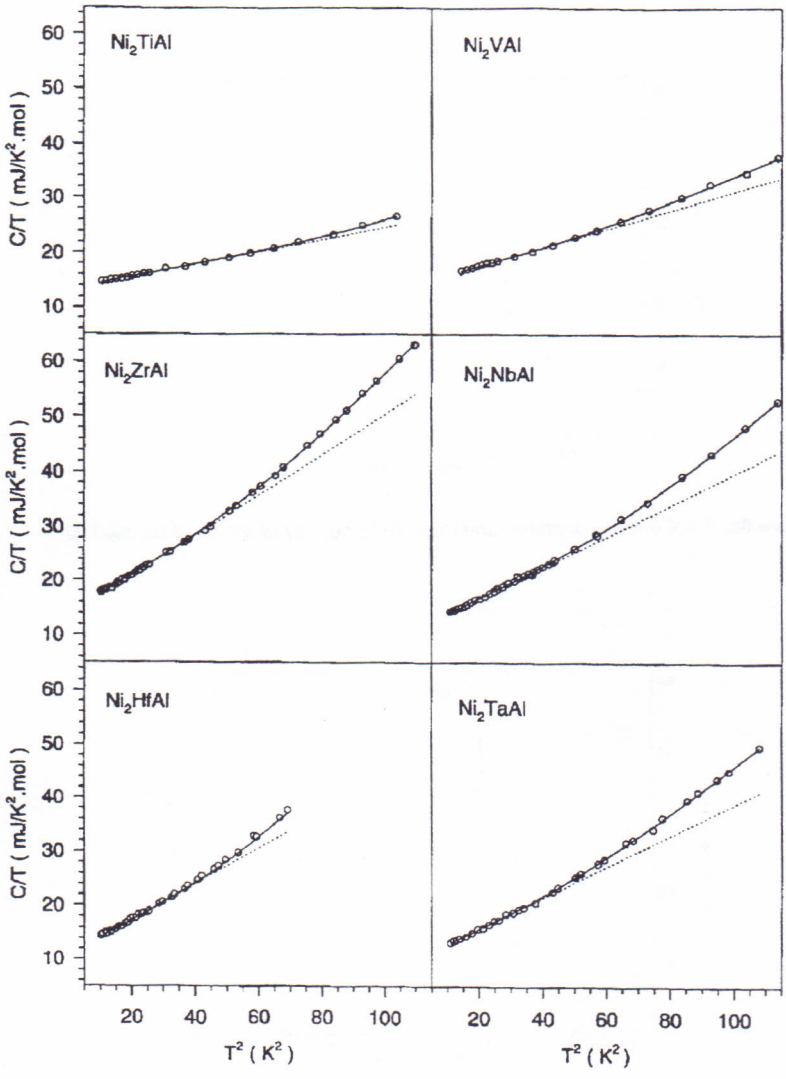

Figure 4: $\frac{C}{T} \times T^2$ plots (O) experimental data; (.....) least squares fits into quation (16) (———) least squares fits into equation (18)

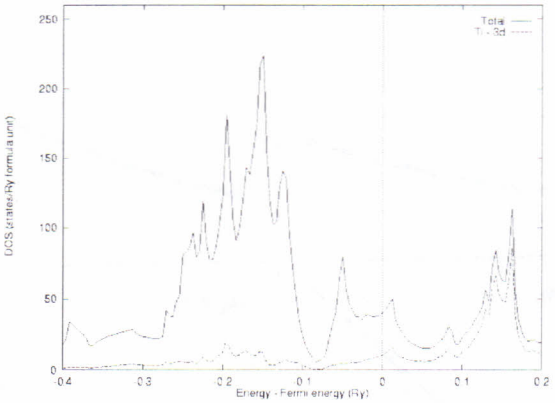

Figure 5a: Total density of states and local Ti-3d density of states of the Ni_2TiAl.

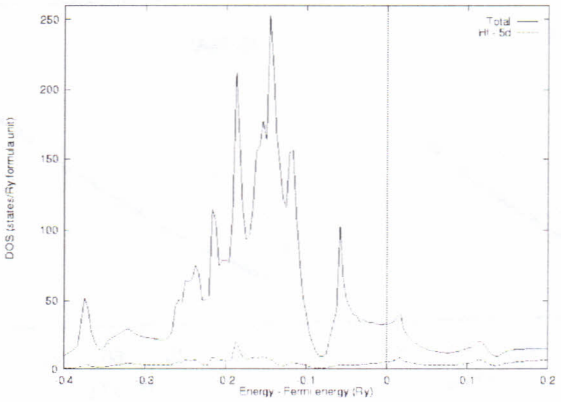

Figure 5b: Total density of states and local Hf-4d density of states of the Ni_2HfAl